photochem

MDPI

Article

Concurrent Photooxidation and Photoreduction of Catechols and Para-Quinones by Chlorophyll Metabolites

Katherine Phan, Emily E. Lessard, Joseph A. Reed, Meredith G. Warsen, Soren Zimmer and Lisa M. Landino *

Department of Chemistry, College of William & Mary, Williamsburg, VA 23815, USA
* Correspondence: lmland@wm.edu

Abstract: Photosynthesis is initiated when the sun's light induces electron transfer from chlorophyll to plastoquinone, a para-quinone. While photosynthesis occurs in the intact chloroplasts of living plants, similar photochemical reactions between dietary chlorophyll metabolites and quinones are likely and may affect health outcomes. Herein, we continue our studies of the direct photoreduction of para-quinones and ortho-quinones that were generated by the photo-oxidation of catechols. Chlorophyll metabolites, including pheophorbide A, chlorin e6, and pyropheophorbide A, as well as methylene blue were employed as photosensitizers. We detected hydrogen peroxide using horseradish peroxidase following the photo-oxidation of the catechol dopamine, even in the presence of EDTA, a tertiary amine electron donor. Under ambient oxygen, hydrogen peroxide was also detected after the photoreduction of several para-quinones, including 2,3-dimethoxy-5-methyl-p-benzoquinone (CoQ_0), methoxy-benzoquinone, and methyl-benzoquinone. The combinations of methylene blue and EDTA or pheophorbide A and triethanolamine as the electron donor in 20% dimethylformamide were optimized for photoreduction of the para-quinones. Chlorin e6 and pyropheophorbide A were less effective for the photoreduction of CoQ_0 but were equivalent to pheophorbide A for generating hydrogen peroxide in photo-oxidation reactions with photosensitizers, oxygen, and triethanolamine. We employed dinitrophenylhydrazine to generate intensely colored adducts of methoxy-benzoquinone, methyl-benzoquinone, and 1,4-benzoquinone.

Keywords: catechol; quinone; singlet oxygen; photoreduction; chlorophyll; pheophorbide a; methylene blue; hydrogen peroxide

Citation: Phan, K.; Lessard, E.E.; Reed, J.A.; Warsen, M.G.; Zimmer, S.; Landino, L.M. Concurrent Photooxidation and Photoreduction of Catechols and Para-Quinones by Chlorophyll Metabolites. *Photochem* **2024**, *4*, 346–360. https://doi.org/10.3390/photochem4030021

Received: 1 July 2024
Revised: 7 August 2024
Accepted: 12 August 2024
Published: 15 August 2024

1. Introduction

Photosynthesis is the light-dependent pathway by which plants consume carbon dioxide and synthesize glucose. Photo-excitation of chlorophyll, the light-harvesting pigment of green plants, initiates electron transfer to plastoquinone, a membrane-bound para-quinone [1]. While considerable research has been devoted to understanding this multi-step and life-sustaining pathway, only limited work has been performed on chlorophyll photoreactivity outside the confines of the chloroplasts in living plants.

Recent research suggests that by consuming green plants, the sun's energy may be used to perform chemical reactions that ultimately influence health, longevity, and even our susceptibility to diseases of aging [2–4]. Qu et al. showed that the combination of chlorophyll derivatives and red light reduced ubiquinone (also called Coenzyme Q) to ubiquinol in vitro [2]. Ubiquinone, a membrane-bound para-quinone nearly identical to plastoquinone, is an essential component of the electron transport chain (ETC) in mitochondria used to produce ATP, and it also functions as a lipid-soluble antioxidant [5,6]. This light-driven reaction of ubiquinone may be a novel mechanism to affect ATP synthesis because cycles of ubiquinone reduction and oxidation are requisite for the proper functioning of the ETC [6]. The redox cycling of ubiquinone resembles that of plastoquinone in chloroplasts during photosynthesis [1].

In support of this, Zhang et al. reported that ATP yield in isolated mouse mitochondria increased when they were combined with the chlorophyll derivative, pyropheophorbide A (ppA), and exposed to red light (670 nm) [4]. In the absence of ppA or red light, no increase in ATP yield was observed. Furthermore, when *C. elegans* samples were fed ppA and exposed to red light, both ATP synthesis and life span increased [3].

Similar experiments performed in mice showed that a diet enriched with chlorophyll metabolites coupled with red light exposure decreased markers of inflammation in those animals, but not in the controls [4]. In treated mice, direct fluorescence imaging showed that chlorophyll metabolites were still photo-excitable and accumulated in multiple cellular locations, including in fat, the brain, and the gut [4].

While increased ATP yield and life span may be attributed to the enhanced photoreduction of ubiquinone, additional components of the ETC or other molecules are likely affected by the combination of red light and chlorophyll derivatives. Our interest was piqued by the structural similarities between the p-quinones, such as plastoquinone and ubiquinone, and catechols. Catechols include plant-derived antioxidants like catechin and EGCG from green tea as well as the neurotransmitters dopamine and epinephrine [7,8]. Catechols function as antioxidants by scavenging reactive oxygen species (ROS) that accumulate as byproducts of normal cellular metabolism [7,9,10].

We reported that catechols can be photo-oxidized by the combination of chlorophyll metabolites, dissolved oxygen, and red light [11]. To study these reactions, we measured rates of dopamine (DA) oxidation to aminochrome (AC) (Scheme 1) [12]. For comparison, we employed methylene blue (MB), a well-characterized photosensitizer. Importantly, we showed that by including an electron donor, we could photoreduce DA that had been oxidized to the o-quinone intermediate, thereby halting the formation of AC. In addition to the colorimetric DA oxidation assay, we observed O_2 uptake as well, both in the absence and presence of the electron donor, consistent with this redox cycling mechanism (Scheme 1).

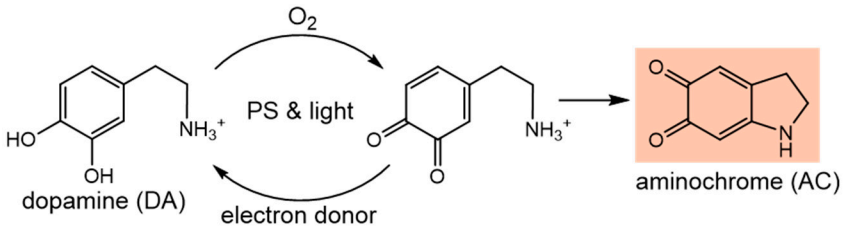

Scheme 1. Photo-oxidation and photoreduction of DA; PS = photosensitizer.

The o-quinone photoreduction step is intriguing because catechol antioxidants and neurotransmitters are oxidized to o-quinones by ever-present ROS [7,9,10]. Photoreduction back to the catechol by the combination of dietary chlorophyll and red light exposure would be a novel mechanism to increase an organism's antioxidant capacity. A requirement for light exposure to maximize health is not unique given that we evolved to depend on ultraviolet light for vitamin D biosynthesis [13].

Furthermore, many naturally occurring p-quinones beyond plastoquinone and ubiquinone may be affected by the combination of chlorophyll and red light. For example, menadione (Vitamin K3) is a naphthoquinone that must be reduced to function in blood coagulation [14]. Aquatic ecosystems often contain chlorophyll from decaying plants and phytoplankton as well as organic materials like humic acids that contain both catechol and p-quinone functional groups [15].

In this work, our goals were two-fold: to identify the O_2 product during catechol photo-oxidation; and to explore the photoreduction of p-quinones under ambient oxygen. Previously, for catechols, we observed photo-oxidation followed by photoreduction [11]. Therefore, for p-quinones, we expect photoreduction to a hydroquinone followed by photo-oxidation. Both cycles are evidence of concurrent photo-oxidation and photoreduction pathways by MB and chlorophyll metabolites.

2. Materials and Methods

All chemicals were from Fisher Scientific or Sigma (St. Louis, MO, USA) and were of the highest purity available. pheoA, ppA, chlorin e6, 1,4-HQ, and all p-quinone stock solutions were prepared in DMF and stored at −20 °C. All other solutions were prepared in water or 10 mM PB pH 7.4. EDTA, TEOA, and TEA stock solutions were adjusted to 7.4 or 8.0 with NaOH or HCl. All buffers were equilibrated to room temperature (20–22 °C) to ensure no differences in dissolved O_2.

2.1. Red Light Specifications

A 36-watt red light composed of 18 2-watt LEDs was used for all photochemical experiments. The maximum wavelength of emitted light was 660 nm. The intensity was quantitated in lux, and intensity as a function of the distance from the light source to the samples was measured to ensure consistent exposure.

2.2. Dopamine Oxidation

Reactions (100 µL) contained 1 mM DA and 2.5 µM in 10 mM PB pH 7.4 in a 96-well plate; the surface of each well was exposed to air under ambient oxygen conditions. Aminochrome (AC) absorbance was measured at 450 nm prior to light exposure and at indicated time intervals. To determine AC concentrations from the plate assay, samples were scanned in a 1 cm pathlength microcuvette to determine a conversion factor at 450 nm because the pathlength in a plate reader format varies by sample volume. AC absorbs at 470–475 nm (3245 M^{-1} cm^{-1}) [16]. EDTA was included to assess effects on AC yield. After 5 min, HRP (2 µL of 50 µM) was added to each well (1 µM final concentration). The increase in absorbance due to H_2O_2 was measured after 2.5 min.

2.3. Oxygen Uptake Assays

Reactions (5 mL) contained 1.0 or 1.5 mM CoQ_0, MB, and EDTA in 10 mM PB pH 7.4 in a 15 mL glass vial. Dissolved oxygen was measured prior to light exposure and at the indicated time intervals using a Mettler-Toledo 605-ISM polarographic dissolved oxygen probe. Reactions were performed under ambient oxygen, and the surface of the solution was exposed to air. The maximum amount of DMF was 7.5% to minimize damage to the electrode components. Absorbance (multiple 100 µL portions) was measured prior to and immediately after light exposure. The change in absorbance at 405 nm was used to calculate the change in CoQ_0 concentration. From the scans of CoQ_0 solutions, we determined a molar absorptivity of 740 M^{-1} cm^{-1}. HRP was added to the portions that had been exposed to light, and the absorbance was reread 2.5 min after HRP addition.

2.4. CoQ_0 Photoreduction Assays

CoQ_0 (1 or 1.5 mM final) was combined with 5 µM MB in water or 25 µM pheoA, ppA, or chlorin e6 in 10 mM PB pH 7.4. EDTA, TEOA, or TEA were added as electron donors. Reactions (100 µL) were irradiated for 5 min for MB and up to 10 min for pheoA, ppA, and chlorin e6 in a 96-well plate. Absorbance was measured at 405 nm (MB) and 450 nm (chlorophyll metabolites) prior to light exposure and at time intervals. Controls with only CoQ_0 or a photosensitizer alone were performed. Dark samples containing all reactants served as controls. For pheoA, ppA, and chlorin e6, the initial photosensitizer absorbance was subtracted to determine the change in CoQ_0 due to its photoreduction. DMF concentrations typically ranged from 10 to 20% for pheoA, ppA, and chlorin e6; the maximum % DMF with MB was 7.5%.

2.5. Detection of p-Quinones with DNPH

Photoreduction reactions with 1,4-BQ, methoxy- and methyl-benzoquinone (100 µL) were prepared as described above for CoQ_0. Aliquots (10 µL) of the dark, light, and light plus HRP samples were combined with 60 µL 1 mM DNPH in 2 M HCl (6-fold excess) for

30 min in the dark. NaOH (2.4 M, 80 µL) was added to yield the deprotonated DNP adduct. Absorbance readings (400–700 nm) were performed immediately after NaOH addition.

2.6. Oxidation of 1,4-HQ to 1,4-BQ by H_2O_2/HRP or MB/Red Light

1,4-HQ (1 mM) was combined with 10 mM PB pH 7.4, 1 mM H_2O_2, and HRP (1 µM final) in 100 µL reactions at room temp. After 5 min, aliquots (2 × 10 µL) were combined with DNPH as described above for p-quinones and quenched with NaOH after 30 min. Absorbance was measured between 400 and 700 nm. The final concentration of DMF was 5%. For photo-oxidation, HQ (1 mM) was combined with 5 µM MB in 10 mM PB pH 7.4 (100 µL) at room temp. The samples were irradiated for 5 min, mixed to re-incorporate dissolved O_2, and irradiated for an additional 5 min. The DNPH procedure was followed to detect the DNP adduct. Authentic 1,4-BQ was also detected by this method.

2.7. Detection of H_2O_2 with TMB and HRP

For reactions containing only photosensitizers and tertiary amines (no CoQ_0), TMB and HRP were used to detect H_2O_2. Aliquots (20 µL) of photochemical reactions were combined with 1 mM TMB and 1 µM HRP in 100 µL. After blue color development, 100 µL of 1 M HCl was added. Absorbance was read at 450 nm in a 96-well plate. A standard curve from 0 to 80 µM H_2O_2 was used to calculate H_2O_2 concentrations in the photochemical reactions.

2.8. Data Analysis

For each treatment/condition, at least three independent experiments were performed in duplicate or triplicate by different researchers using different micropipettes. Mean values were calculated for each independent experiment (mean ± error). For figures showing error bars, mean values were averaged and the error was calculated. Details for each are stated in the figure legends.

3. Results

In our recent work describing the photo-oxidation and photoreduction of catechols using MB and chlorophyll metabolites as photosensitizers, we observed O_2 uptake during photo-oxidation of DA to AC but did not identify the O_2 product [11]. Herein, we provide evidence that catechol photo-oxidation to the o-quinone proceeds through $^1O_2$-mediated hydrogen atom abstraction to yield a peroxyl radical, •OOH. The pK_a of •OOH is 4.8; therefore, at neutral pH, it will deprotonate to superoxide anion [17]. Disproportionation of two superoxide anions yields O_2 and H_2O_2 according to Equation (1). Furthermore, two resulting catechol semiquinones (RO•) disproportionately yield an o-quinone and regenerate a catechol [18]. Thus, the ratio of products, from o-quinone (and consequently AC) to H_2O_2, should be 1:1.

$$O_2^{-\bullet} + O_2^{-\bullet} + 2H^+ \rightarrow H_2O_2 + O_2 \quad (1)$$

To test for H_2O_2, HRP was added following DA photo-oxidation to AC (Figure 1). HRP uses H_2O_2 to oxidize many organic molecules, including catechols and hydroquinones [19,20]. Because DA is oxidized by HRP only when H_2O_2 is available, AC further increased after HRP was added (the solution contained sufficient unreacted DA). If catalase, an enzyme that also consumes H_2O_2, was added prior to HRP, no increase in AC was detected. Catalase reacts according to Equation (2):

$$2H_2O_2 \rightarrow 2H_2O + O_2 \quad (2)$$

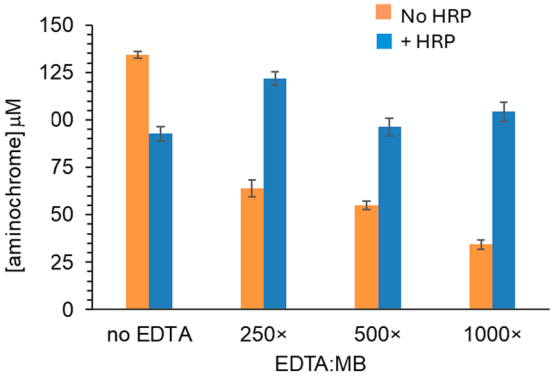

Figure 1. Photo-oxidation of DA to aminochrome; detection of H_2O_2 with HRP reactions (100 µL) contained 1 mM DA, 2.5 µM MB, and varying EDTA in 10 mM PB pH 7.4 in a 96-well plate under ambient oxygen. Absorbance at 450 nm was measured prior to and after irradiation. For +HRP samples, HRP (1 µM final) was added, and color development was measured after 2.5 min. The data shown are the average of three independent experiments performed in duplicate.

Figure 1 also shows that the inclusion of EDTA led to a dose-dependent decrease in AC yield, consistent with our prior work (−HRP). Even though less AC was produced, H_2O_2 production was not halted by EDTA. For all EDTA concentrations tested, the yield of H_2O_2 was greater than if no EDTA was present. High ratios of EDTA to MB were critical to ensure the transfer of electrons from EDTA to MB so that MB continues to photoreduce additional o-quinone intermediates.

Although increased AC after HRP addition confirmed that photo-oxidation produced H_2O_2, exact quantitation was not possible. AC is not stable in aqueous solution at neutral pH, and some of its rearrangement products, including leukoaminochrome and 5,6-dihydroxyindole, are also HRP co-substrates [21,22]. To confirm this in our system, DA (1 mM), HRP, and a known amount of H_2O_2 were combined to generate ~200 µM AC. When a second equal amount of H_2O_2 was added, the increase in AC was less than for the first amount, even though the solution containing unreacted DA and HRP was still active. This proves that solutions of orange AC contained other substances that also act as HRP co-substrates. HRP assays for H_2O_2 using other peroxidase co-substrates, including ABTS, o-phenylenediamine, and TMB, were unsuccessful because excess DA, AC, and its rearrangement products in the solution prevented their color formation.

H_2O_2 formation, even when EDTA was present, supports our hypothesis of concurrent photo-oxidation of DA by $^1O_2$ to the intermediate o-quinone, followed by photoreduction back to DA by the combination of red light, MB, and EDTA (Scheme 1). If both pathways occurred concurrently with DA (oxidation followed by o-quinone reduction), we suspected that a p-quinone could be reduced to its hydroquinone form and then be re-oxidized by $^1O_2$ (Scheme 2).

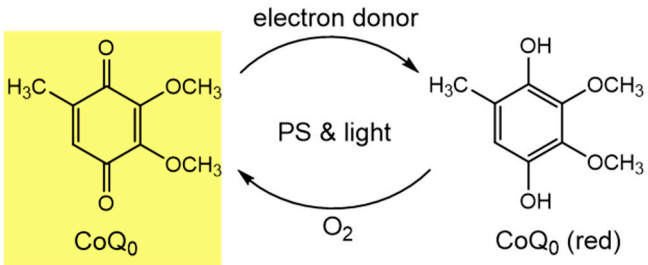

Scheme 2. Photoreduction and photo-oxidation of CoQ_0.

To address this, we revisited the CoQ_0 photoreduction assay that we employed in our prior work [11]. CoQ_0 is an analog of CoQ_{10} but is more water soluble, though some DMF is required. For CoQ_0, there is a color change from yellow to colorless upon reduction that

is easily monitored by UV/Vis spectroscopy or in a 96-well plate format. If cycling from oxidized p-quinone to hydroquinone and back to p-quinone occurs, then we would expect an oxygen uptake as CoQ_0 is photoreduced under ambient oxygen.

For O_2 uptake measurements, larger sample volumes are required to accommodate the O_2 probe; thus, the time course of photochemical reactions is different from samples prepared in a 96-well plate. In Figure 2A, changes in both dissolved O_2 and CoQ_0 concentrations are shown. For both 1.0 and 1.5 mM CoQ_0, the extent of photoreduction and the decrease in O_2 concentration were identical. Given that the concentrations of MB, dissolved O_2, and EDTA were identical, this result was expected. Even in the absence of CoQ_0, O_2 uptake was observed, though it was lower than for the samples with CoQ_0. For the $-CoQ_0$ samples, the addition of up to 7.5% DMF did not affect O_2 uptake.

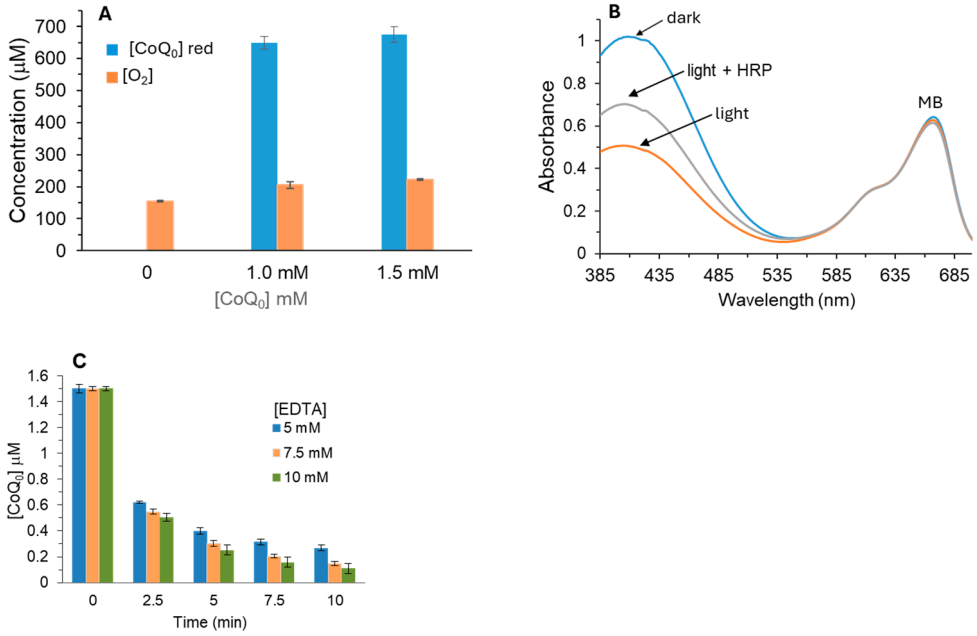

Figure 2. Photoreduction of CoQ_0 by MB/EDTA; O_2 uptake and detection of H_2O_2 with HRP. (**A**) Reactions (5 mL) contained 5 μM MB, 5 mM EDTA in 10 mM PB pH 7.4. Reactions with CoQ_0 contained either 5% DMF (for 1.0 mM) or 7.5% DMF (for 1.5 mM). The sample without CoQ_0 contained up to 7.5% DMF. Absorbance values at 405 nm before and after irradiation (5 min) were used to determine the [CoQ_0] reduced. O_2 readings were taken before and after light. These data are the average of at least three independent experiments. (**B**) Reactions were prepared as in (**A**). Visible scans of 100 μL aliquots were taken before and after 5 min of light. HRP (1 μM final) was added to light samples and scanned after 2.5 min. Scans are the averages of two samples each performed in duplicate. (**C**) Reactions (100 μL) contained 5 μM MB and varying EDTA in 10 mM PB pH 7.4. The absorbance at 405 nm was measured prior to light and at indicated times. These data are the average of three independent experiments performed in triplicate.

Tertiary amines like EDTA are known to react with $^1O_2$, but at much lower rates than hydroquinones [23–25]. Therefore, in the absence of CoQ_0, or when CoQ_0 hydroquinone is not yet available, the reaction of $^1O_2$ with EDTA produces the amine cation radical and $O_2^{-\bullet}$ according to Equation (3).

$$^1O_2 + R_3N: \rightarrow O_2^{-\bullet} + R_3N^{+\bullet} \quad (3)$$

When CoQ_0 hydroquinone is available, it will be oxidized to a semiquinone via the same hydrogen atom abstraction process as for $^1O_2$ oxidation of DA. Thus, $^1O_2$ reacts with both EDTA or CoQ_0 hydroquinone to produce H_2O_2. In Figure 2A, the greater O_2 uptake when CoQ_0 is present supports cycles of photoreduction to hydroquinone, followed by its

reoxidation given the much higher rate constants for the reaction of hydroquinones with $^1O_2$ relative to tertiary amines like EDTA [23,24].

For identical O_2 uptake reactions, H_2O_2 was measured using HRP. The CoQ_0 hydroquinone is a co-substrate for HRP, and oxidation restores its absorbance at 405 nm (Figure 2B). Unlike DA oxidation to AC in Figure 1, there are no secondary products that skewed our interpretation.

Figure 2B shows UV/Vis scans of CoQ_0 photoreduction reactions before irradiation after 5 min of red light and for light samples with added HRP. Following irradiation, the peak at 405 nm corresponding to CoQ_0 decreased due to photoreduction. When HRP was added, some absorbance at 405 nm was restored. If catalase was added prior to HRP, no increase in absorbance was detected because catalase consumes the requisite H_2O_2 (Equation (2)). No changes at lower wavelengths were observed. The second peak at ~665 nm corresponds to MB, and no photobleaching occurred after 5 min of light exposure. No oxygen uptake was observed for MB and CoQ_0 in the absence of EDTA. This result confirms that H_2O_2 was produced during CoQ_0 photoreduction under ambient oxygen.

The CoQ_0 photoreduction reaction with MB was optimized for EDTA concentration and reaction time. We sought to determine the lowest EDTA concentration required so as to minimize its reaction with $^1O_2$. Figure 2C shows that for all three EDTA concentrations tested, at least 60% of the 1.5 mM CoQ_0 was photoreduced after 2.5 min. While photoreduction with 7.5 and 10 mM EDTA was superior to 5 mM at all times tested, there was little change in CoQ_0 concentration after 5 min regardless of EDTA concentration. With 1.5 mM CoQ_0 and only 5 μM MB, the maximum number of turnovers was 300 (ratio of CoQ_0:MB) [11].

Additional CoQ_0 photoreduction assays with 5 μM MB and 5 mM EDTA were performed in a 96-well plate to determine H_2O_2 concentrations at different time intervals. Again, we used HRP to convert the photoreduced CoQ_0 (colorless) back to the yellow oxidized p-quinone. Corresponding reactions without CoQ_0 were also analyzed for H_2O_2 using TMB and HRP. Table 1 shows that at all times tested, the concentration of H_2O_2 was greater when CoQ_0 was included. This is consistent with the O_2 uptake data in Figure 2A. In Figure 2A, using a 5 mL volume in a glass vial, the change in O_2 concentration was ~220 μM after 5 min. In the 96-well format, the surface of the 100 μL reactions is exposed to air; therefore, as dissolved O_2 is depleted, additional H_2O_2 still forms at the solution/air interface. This is evident in the greater than 300 μM H_2O_2 values observed for all +CoQ_0 samples. Of note, the average concentration of dissolved O_2 at 20–22 °C was ~300 μM.

Table 1. H_2O_2 yield by MB/EDTA in μM after red light exposure.

Time (min)	+1.5 mM CoQ_0 (μM)	−CoQ_0 (μM)
1.5	334 ± 10	80 ± 2
2.5	421 ± 11	108 ± 1
5	524 ± 17	126 ± 2 [1]

[1] All samples contained 5 μM MB and 5 mM EDTA in 10 mM PB pH 7.4. Samples with CoQ_0 contained 7.5% DMF. The addition of 7.5% DMF to −CoQ_0 samples did not alter H_2O_2 yield. The data shown are the averages of at least two independent experiments performed in triplicate. The error is the standard deviation.

To investigate the reactivity of chlorophyll metabolites as photosensitizers, we examined CoQ_0 photoreduction with varying electron donors and with differing amounts of DMF. In our prior work, EDTA had very limited reactivity with pheoA, the major chlorophyll metabolite expected after consumption of green plants [26,27]. Furthermore, chlorophyll metabolites are less soluble necessitating additional DMF (up to 20%) relative to MB, whose reactions only contain 5–7.5% DMF because CoQ_0 stock solutions were prepared with it.

To optimize photoreduction under ambient oxygen conditions, we varied the % DMF for CoQ_0 photoreduction by pheoA and TEOA. First, we examined the effect of 5–20% DMF on the absorbance of pheoA in PB pH 7.4 or pH 8.0 at 667 and 685 nm; these wavelengths

correspond to the monomer and dimer forms of pheoA, respectively [28]. We observed a distinct shift from 685 to 667 nm as the % DMF increased from 5 to 20% (Supplemental Figure S1). For subsequent assays with pheoA, CoQ_0, and TEOA, the extent of photoreduction also increased with increasing DMF. The increase in activity was most prominent between 15 and 20% DMF, with an increase from ~30 to 51 turnovers with a constant ratio of TEOA to pheoA (2000:1) at pH 8.0. We did not test higher DMF concentrations because the shift from dimer to monomer was nearly complete with 20% DMF. Furthermore, we did not want higher DMF to compromise the activity of enzymes, including HRP, SOD, and catalase, that we use to elucidate photo-oxidation and photoreduction pathways.

Both TEOA and TEA were tested as electron donors for CoQ_0 photoreduction with 25 µM pheoA in 20% DMF. Figure 3A shows the time course of CoQ_0 photoreduction at pH 7.4 and 8.0. For both TEOA and TEA, pH 8.0 was superior to pH 7.4. Because TEOA and TEA concentrations are 50 mM, their pH dominates that of the entire solution, effectively acting as the buffer. Because only deprotonated tertiary amines can function as electron donors, this is consistent with their pK_a values of 7.75 and 10.7 for TEOA and TEA, respectively. Given our interest in pheoA photoreactivity under physiological conditions, we did not test higher pH values.

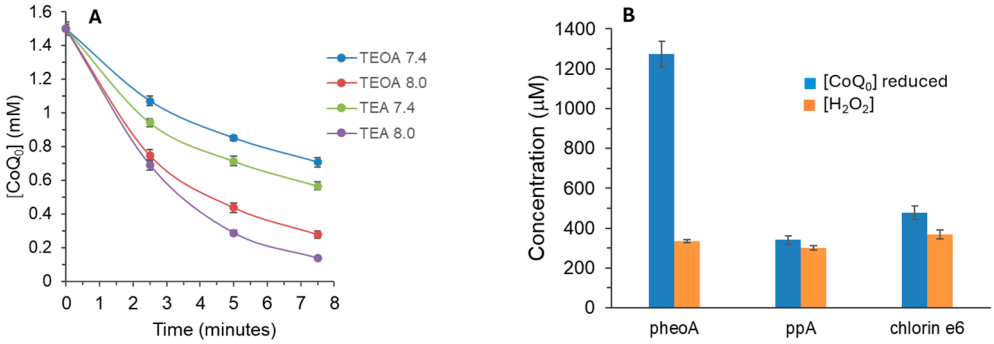

Figure 3. Photoreduction of CoQ_0 by chlorophyll metabolites. (**A**) Reactions (100 µL) contained 25 µM pheoA, 50 mM electron donor, and 20% DMF in 10 mM PB. The pH of the resulting solution was determined by the electron donor. Absorbance at 450 nm was recorded prior to light exposure and at t = 7.5 min. Controls without CoQ_0 were performed to determine pheoA absorbance at 450 nm prior to and after light. The data shown are the average of three independent experiments performed in duplicate. (**B**) Reactions (100 µL) contained 25 µM pheoA, ppA, or chlorin e6; 50 mM TEOA pH 8.0; and 20% DMF in PB. Absorbances of CoQ_0 and pheoA controls were measured as in (**A**). H_2O_2 (−CoQ_0) was measured after 5 min of light. Aliquots (20 µL) were combined with 10 mM PB pH 7.4, 1 mM TMB, and 1 µM HRP (100 µL total). Reactions were quenched with 100 µL of 1 M HCl, and the absorbance was measured at 450 nm. These data are the average of three independent experiments performed in duplicate.

At 7.5 min, ~85% and 92% of 1.5 mM CoQ_0 was reduced for the TEOA and TEA samples at pH 8.0, respectively. This corresponds to at least 50 turnovers for pheoA (mol CoQ reduced/mol pheoA), which is more than 2-fold greater than the maximum number of 18–20 that we reported previously [11]. Furthermore, following CoQ_0 photoreduction under ambient oxygen, we tested for H_2O_2 using HRP. Regardless of pH or electron donor, we observed an increase in CoQ_0 absorbance after HRP addition, as we had observed for MB (Figure 2B).

In addition to pheoA, we tested the chlorophyll metabolites, pyropheophorbide (ppA) and chlorin e6, in our CoQ_0 photoreduction assay. For pheoA, we explored the requirement for DMF, varying pH values and the electron donor. No CoQ_0 photoreduction was observed for ppA or chlorin e6 with EDTA as the electron donor (same ratios of EDTA:photosensitizer). Although both TEOA and TEA were effective as electron donors for ppA and chlorin e6, the extent of CoQ_0 photoreduction was much lower than for pheoA (Figure 3B).

Given the differences in photoreduction activity, we compared the amount of H_2O_2 produced by each in the absence of CoQ_0 but with the same tertiary amine (TEOA) and % DMF. Figure 3B shows that ppA and chlorin e6 were equal to or better than pheoA in producing H_2O_2. While TEA was ~20–25% more effective than TEOA for CoQ_0 photoreduction with both ppA and chlorin e6, the extent of photoreduction did not approach that of pheoA.

We examined H_2O_2 yield by pheoA both in the presence and absence of CoQ_0 using the optimized photoreduction conditions. Table 2 shows that at all times tested, more H_2O_2 was detected for the $+CoQ_0$ samples relative to the $-CoQ_0$ samples. This is consistent with our MB results (Table 1). Because higher concentrations of TEOA (50 mM) were employed with pheoA relative to that of EDTA (5 mM) used with MB, the yields of H_2O_2 are all higher. Thus, the reactivity of CoQ_0—with respect to photoreduction and subsequent reoxidation by $^1O_2$—is the same regardless of the photosensitizer and tertiary amine combination.

Table 2. H_2O_2 yield by pheoA/TEOA after red light exposure.

Time (min)	+1.5 mM CoQ_0 (μM)	−CoQ_0 (μM)
2.5	410 ± 27	271 ± 5
5	575 ± 6	334 ± 8
7.5	635 ± 53	394 ± 10

All samples contained 25 μM pheoA, 20% DMF, and 50 mM TEOA pH 8.0. The data shown are the average of at least two independent experiments performed in triplicate. The error is the standard deviation.

Additional CoQ_0 photoreduction experiments were performed to test the effects of catalase, superoxide dismutase (SOD), and a N_2 atmosphere. Catalase slowed the rate of CoQ_0 photoreduction, but SOD had no effect. By regenerating O_2, catalase favors the formation of more $^1O_2$ that will subsequently re-oxidize CoQ_0 hydroquinone (Scheme 2 and Equation (2)). In support of this, we also observed that catalase increased the rate and extent of DA oxidation to AC by increasing O_2 and therefore $^1O_2$.

SOD had no effect on CoQ_0 photoreduction because it only accelerates the already rapid nonenzymatic disproportionation of $O_2^{-\bullet}$ to form O_2 and H_2O_2 (Equation (1)) [29]. Neither enzyme was present in sufficient quantity to act as a $^1O_2$ scavenger via the oxidation of protein amino acids [30]. When CoQ_0 photoreduction reactions were bubbled with N_2 for up to 60 s to displace dissolved O_2, the rate of photoreduction increased by 10–20%, and the yield of H_2O_2 decreased by as much as 50%.

We compared CoQ_0 photoreactivity with other p-quinones, including 1,4-benzoquinone (1,4-BQ), methoxy-benzoquinone (mBQ), and methyl-benzoquinone (methylBQ). Both MB/EDTA and pheoA/TEOA/DMF conditions were employed for photoreduction. Because these p-quinones do not absorb in the visible range, we used DNPH as a derivatizing agent that reacts with the p-quinones but not with the reduced hydroquinones. Under basic conditions, these DNP adducts absorbed between 543 nm (for mBQ) and 513 nm (for 1,4-BQ).

Figure 4 shows the dark, light, and light + HRP samples of mBQ analogous to those in Figure 2B after derivatization with DNPH. Irradiation of mBQ resulted in photoreduction, thus decreasing the yield of the DNP adduct. The addition of HRP regenerated some of the mBQ DNP adduct because, as for CoQ_0, H_2O_2 was produced during photoreduction under ambient oxygen, and because mBQ is an HRP co-substrate. The addition of catalase prior to HRP abolished the increase in mBQ DNP adduct. While the samples in Figure 4 were prepared using MB and EDTA, identical results were obtained with pheoA and TEOA.

For methylBQ, we also observed a decrease in DNP adduct for the light sample and an increase in the DNP adduct when HRP was added. Supplementary Figure S2 shows the dark, light, and light + HRP samples of methylBQ using pheoA and TEOA with 20% DMF (same conditions as for CoQ_0 in Figure 3A). The absorbance maximum of the methylBQ DNP adduct was 532 nm vs. 543 nm for mBQ.

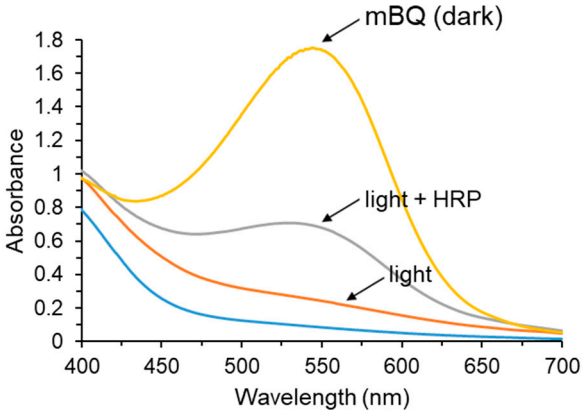

Figure 4. Photoreduction of mBQ and detection of its DNP adduct. Reactions (100 µL) contained 5 µM MB, 5 mM EDTA, and 1.0 mM mBQ in 10 mM PB pH 7.4. Aliquots (10 µL) of the dark, light, and light plus HRP samples were combined with 6-fold excess DNPH in 2 M HCl for 30 min in the dark. Absorbance readings (400–700 nm) were performed immediately after NaOH addition. The representative data shown are average scans performed in duplicate. DNPH alone is shown in blue.

Lastly, we used DNPH derivatization to confirm the oxidation of 1,4-hydroquinone (1,4-HQ) to 1,4-BQ. Our results herein are based on the known reactions of hydroquinones with both $^1O_2$ and HRP/H_2O_2 to yield the corresponding p-quinones [23,31,32]. 1,4-HQ is stable and commercially available, unlike the reduced forms of CoQ_0, mBQ, and methylBQ.

Figure 5 shows that the visible spectrum of the DNP adduct of authentic 1,4-BQ is identical to that of 1,4-HQ treated with H_2O_2 and HRP. As expected, the extent of 1,4-HQ oxidation was dependent on the concentration of H_2O_2 (blue curve). When 1,4-HQ was photo-oxidized with MB and red light under ambient oxygen and subsequently modified with DNPH, the same DNP adduct was produced (yellow curve).

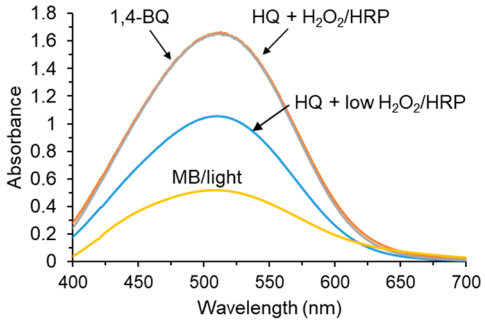

Figure 5. Oxidation of 1,4-HQ by H_2O_2/HRP or photo-oxidation with MB/light/O_2. 1,4-HQ (1 mM) was combined with 0.5 or 1 mM H_2O_2 and HRP (1 µM final) in 10 mM PB pH 7.4. For photo-oxidation, 1,4-HQ (1 mM) was combined with 5 µM MB in 10 mM PB pH 7.4 at room temp. Samples were irradiated for 5 min, mixed to increase dissolved O_2, and irradiated again for 5 min. 1,4-BQ was detected with DNPH as described for p-quinones. The representative data shown are average scans performed in duplicate.

4. Discussion

Our previous work on catechol photo-oxidation provided clear evidence for $^1O_2$ as the oxidant responsible for DA oxidation to AC [11]. Inhibition by azide and enhanced oxidation in D_2O are hallmarks of $^1O_2$-mediated reactions [33,34]. Because O_2 uptake was observed following photo-oxidation of DA, a model catechol, we sought to identify the resulting product formed from O_2.

Herein, we showed that H_2O_2 is produced during DA photo-oxidation by employing HRP, an enzyme that reacts with H_2O_2 and DA (Figure 1). HRP can only increase AC yield after photo-oxidation if H_2O_2 is present. When catalase consumed H_2O_2 (Equation (2))

prior to HRP addition, no increase in AC yield was detected, further confirming the presence of H_2O_2 after photo-oxidation. Both catechols and hydroquinones (reduced p-quinones) are HRP co-substrates; therefore, H_2O_2 was successfully confirmed via direct color changes in our existing DA photo-oxidation and CoQ_0 photoreduction assays (Schemes 1 and 2) [22,31,32,35]. Hydrogen atom abstraction by $^1O_2$ also explains the formation of the intermediate o-quinone. The disproportionation of resulting semiquinones (RO•) yields an o-quinone and regenerates catechol [18].

This work also confirms that DA photo-oxidation to the intermediate o-quinone and subsequent photoreduction occurred when both O_2 and an electron donor were present (Scheme 1). Increasing the EDTA (with constant MB) increased CoQ_0 photoreduction (Figure 2). Indeed, we optimized CoQ_0 turnovers using MB and EDTA from 180 to 200 in our prior work to ~300 (mol CoQ_0 reduced/mol MB) [11].

Tertiary amines including EDTA, TEOA, and TEA are well-established electron donors in photoreduction systems [36,37]. However, their reactions with $^1O_2$ (Equation (3)) to produce H_2O_2 is central to our data interpretation. EDTA may scavenge $^1O_2$, thereby competing with DA for it; however, the rate constant for $^1O_2$ and EDTA is only ~10^5 M^{-1} s^{-1} [24]. By contrast, the rate constant for catechols and $^1O_2$ is at least 2–3 orders of magnitude greater (Table 3).

Table 3. Relevant rate constants [1] for oxidation with $^1O_2$.

Reaction	Rate Constant (M^{-1} s^{-1})	Reference
Catechols + $^1O_2$	~10^8	[38]
Hydroquinones + $^1O_2$	~10^7–10^8	[23]
EDTA + $^1O_2$	~10^5	[24]

[1] Solvent conditions are not identical to those used herein.

For example, in Figure 1, the highest EDTA concentration tested was 2.5 mM, while for DA, it was 1 mM. Given the substantial difference in rate constants, it is clear that under these conditions, $^1O_2$ will react with DA, not EDTA. However, in the absence of catechol or hydroquinone, tertiary amines react with $^1O_2$ and also produce H_2O_2 (Tables 1 and 2). A reaction between EDTA and $^1O_2$ is likely when CoQ_0 photoreduction is first initiated and O_2 is plentiful. As the CoQ_0 hydroquinone accumulates, $^1O_2$ will oxidize it, not EDTA. Given that both oxidation events yield H_2O_2, it is not possible to quantify each separately.

The chlorophyll metabolites studied herein—pheoA, ppA, and chlorin e6—photoreduced CoQ_0 and also produce H_2O_2 (Figure 3). This is important because chlorophyll metabolites reacted like MB, a well-characterized synthetic photosensitizer [39]. However, unlike MB, which is positively charged at neutral pH, EDTA was not effective as an electron donor with pheoA, ppA, or chlorin e6. pheoA and ppA have one negative carboxylate at neutral pH, whereas chlorin e6 has three [11,40,41]. Therefore, due to charge repulsion, we did not expect to observe electron transfer from EDTA, with its multiple carboxylates, to any of them [41]. Even with TEAO and TEA as electron donors (and no charge repulsion), pheoA turnovers (mol CoQ_0 reduced/mol pheoA) were consistently lower than MB (~50 vs. 300) (Figures 2C and 3B).

Nonetheless, differences in the reactivity of the three chlorophyll metabolites were observed. pheoA was superior to ppA and chlorin e6 with respect to CoQ_0 photoreduction, but all three generated roughly equal amounts of H_2O_2 (Figure 3B). Chlorin e6 was developed for photodynamic therapy (PDT), wherein red light and a photosensitizer generate $^1O_2$ and other ROS as a means to selectively target cancer cells [40–42]. For PDT, photoreduction would not be a desired outcome, only photo-oxidation [40]. The reasons for the differing reactivities of the three chlorophyll metabolites are not clear, although we speculate that ppA and chlorin e6 may have decreased the capacity to accept electrons from TEOA or TEA relative to pheoA.

As in our prior work, we saw an absolute requirement for an organic solvent—in this case DMF—to enhance pheoA solubility and therefore reactivity. Though TEOA has a much

lower pK_a value (7.75) than TEA (~10.7), TEA was equal to TEOA in our photoreduction system (Figure 3A). This suggests that electron donation to pheoA may be hindered by the hydroxyl groups of TEOA. Given that pheoA is hydrophobic requiring at least 20% DMF for optimal photoreduction, polar hydroxyl groups on TEOA may limit electron transfer.

H_2O_2 yield by both MB/EDTA and pheoA/TEOA was greater when CoQ_0 was present (Tables 1 and 2). This is only possible if CoQ_0 is cycling as depicted in Scheme 2. For this reason, photoreduction turnover numbers (mol CoQ_0 reduced/mol photosensitizer) are not the true measure of total photosensitizer reactivity as its excited state also reacts with O_2 to produce $^1O_2$, though they are commonly reported, even for systems where both photoreduction and $^1O_2$ formation occur [43].

Concurrent photo-oxidation and photoreduction also occurs in intact chloroplasts. Chlorophyll will trigger $^1O_2$ formation (and other ROS products) when light intensity is excessive [44]. Typically, $^1O_2$ is quenched by pigments such as β-carotene and α-tocopherols [33,44]. Thus, even in intact plants, chlorophyll functions in both photo-oxidation and photoreduction pathways.

This work also shows that DNPH conjugation (Figures 4 and 5) is an effective method to study p-quinones that do not absorb strongly in the visible range. DNP adducts are easy to prepare and absorb strongly in the visible range under basic conditions. For example, in Figure 4, the mBQ DNP adduct (only ~67 μM) has an absorbance greater than 1.5. DNPH labeling was also successfully employed to prove that the stable hydroquinone, 1,4-HQ, was oxidized to 1,4-BQ by H_2O_2/HRP and photochemically oxidized by $^1O_2$ (Figure 5).

pheoA photoreactivity is of greatest interest because it is the likely metabolite formed in vivo after eating green plants; therefore, it has health implications [26,27]. While tertiary amines are not relevant electron donors in vivo, the range of photochemical reactions by chlorophyll metabolites beyond the confines of intact chloroplasts has not been explored in any detail. Even if electron donors are limited in vivo, a single photoreduction event by a chlorophyll metabolite may be sufficient to increase catechol antioxidant capacity or favor CoQ_0 hydroquinone, thereby increasing ATP yield [3].

To the best of our knowledge, azobenzenes are the only other class of molecules reported to be photoreduced by chlorophyll metabolites [43]. Dutta et al. employed tin-substituted ppA in conjunction with red light and EDTA to reduce azobenzenes on a nucleic acid template [43].

Our systems involving both o- and p-quinones are also interesting because photoreduction proceeds, even when O_2 is present. Some photoreduction systems designed to produce hydrogen gas only function under a strict anaerobic environment [36].

Lastly, our work suggests a possible aqueous photochemical system to generate H_2O_2. The current industrial process relies on a Pd catalyst, H_2 and O_2 gases, anthraquinone as a redox cycler, and a mixture of organic solvents [45,46]. Herein, we generated H_2O_2 using MB, EDTA, mild red light, and ambient O_2 in neutral aqueous solution (Table 1). Indeed, the yield of H_2O_2 increased when a p-quinone was present that could cycle from oxidized to reduced and back to the oxidized form. The limiting factor was dissolved O_2, which could be readily increased by bubbling the solution with air or O_2 gas. Both EDTA and MB are very water soluble and nontoxic. The only organic solvent required when MB was employed as the photosensitizer was the solvent needed to dissolve the p-quinone. Thus, the project we designed to understand the health benefits of chlorophyll ingestion may be relevant to the critically important industrial process of H_2O_2 synthesis.

5. Conclusions

These results are consistent with our proposed mechanism of CoQ_0 photoreduction and subsequent photo-oxidation of the resulting hydroquinone by $^1O_2$ (Scheme 2). This is further support for the photo-oxidation of DA by $^1O_2$ followed by the photoreduction of the transient o-quinone (Scheme 1). Our methodology employing HRP to detect H_2O_2 after DA photo-oxidation and after CoQ_0 photoreduction assays relies on a straightforward color change (Figures 1 and 2). In addition to CoQ_0, several other p-quinones were photoreduced

using both MB and chlorophyll metabolites as photosensitizers. DNPH derivatization was successfully employed to modify p-quinones so that their photoreduction could be readily measured. This research on chlorophyll photochemistry is intriguing because many natural products that we consume contain catechol and p-quinone functionalities.

Supplementary Materials: The following supporting information can be downloaded at: https://www.mdpi.com/article/10.3390/photochem4030021/s1, Figure S1: Effect of DMF on pheoA absorbance; Figure S2: Photoreduction of methylBQ with pheoA and TEOA; derivatization with DNPH.

Author Contributions: K.P.: methodology, investigation, figure preparation. E.E.L.: methodology, investigation, figure preparation. J.A.R.: methodology, investigation, figure preparation. M.G.W.: methodology, investigation. S.Z.: methodology, investigation. L.M.L.: conceptualization, methodology, investigation, formal analysis, writing—original draft preparation, writing—review and editing, supervision, project administration. All authors have read and agreed to the published version of the manuscript.

Funding: This research received no external funding.

Data Availability Statement: Raw data, procedures, and all Excel files are available upon request.

Acknowledgments: This work was supported by undergraduate summer research awards to K.P. and J.A.R. by the Charles Center at William & Mary. The authors also acknowledge Chris Abelt and Bill McNamara for helpful discussions.

Conflicts of Interest: The authors declare no conflicts of interest.

Abbreviations

AC, aminochrome; 1,4-BQ, 1,4-benzoquinone; CoQ_0, 2,3-Dimethoxy-5-methyl-p-benzoquinone; DA, dopamine; DNPH, dinitrophenylhydrazine; EDTA, ethylenediaminetetraacetic acid; HRP, horseradish peroxidase; 1,4-HQ, 1,4-hydroquinone; MB, methylene blue; mBQ, methoxy-1,4-benzoquinone; methylBQ, methyl-1,4-benzoquinone; pheoA, pheophorbide A; ppA, pyropheophorbide; TEA, triethylamine; TEOA, triethanolamine; TMB, 3,3′,5,5′-tetramethylbenzidine; PB, phosphate buffer; PS, photosensitizer; SOD, superoxide dismutase.

References

1. Havaux, M. Plastoquinone in and beyond Photosynthesis. *Trends Plant Sci.* **2020**, *25*, 1252–1265. [CrossRef] [PubMed]
2. Qu, J.; Ma, L.; Zhang, J.; Jockusch, S.; Washington, I. Dietary Chlorophyll Metabolites Catalyze the Photoreduction of Plasma Ubiquinone. *Photochem. Photobiol.* **2013**, *89*, 310–313. [CrossRef] [PubMed]
3. Xu, C.; Zhang, J.; Mihai, D.M.; Washington, I. Light-Harvesting Chlorophyll Pigments Enable Mammalian Mitochondria to Capture Photonic Energy and Produce ATP. *J. Cell Sci.* **2014**, *127*, 388–399. [CrossRef] [PubMed]
4. Zhang, D.; Robinson, K.; Mihai, D.M.; Washington, I. Sequestration of Ubiquitous Dietary Derived Pigments Enables Mitochondrial Light Sensing. *Sci. Rep.* **2016**, *6*, 34320. [CrossRef] [PubMed]
5. Lee, B.-J.; Huang, Y.-C.; Chen, S.-J.; Lin, P.-T. Coenzyme Q10 Supplementation Reduces Oxidative Stress and Increases Antioxidant Enzyme Activity in Patients with Coronary Artery Disease. *Nutrition* **2012**, *28*, 250–255. [CrossRef] [PubMed]
6. Alcázar-Fabra, M.; Navas, P.; Brea-Calvo, G. Coenzyme Q Biosynthesis and Its Role in the Respiratory Chain Structure. *Biochim. Biophys. Acta (BBA) Bioenerg.* **2016**, *1857*, 1073–1078. [CrossRef]
7. Bolton, J.L.; Dunlap, T.L.; Dietz, B.M. Formation and Biological Targets of Botanical O-Quinones. *Food Chem. Toxicol.* **2018**, *120*, 700–707. [CrossRef]
8. Bolton, J.L.; Dunlap, T. Formation and Biological Targets of Quinones: Cytotoxic versus Cytoprotective Effects. *Chem. Res. Toxicol.* **2017**, *30*, 13–37. [CrossRef]
9. Shimizu, T.; Nakanishi, Y.; Nakahara, M.; Wada, N.; Moro-oka, Y.; Hirano, T.; Konishi, T.; Matsugo, S. Structure Effect on Antioxidant Activity of Catecholamines toward Singlet Oxygen and Other Reactive Oxygen Species in Vitro. *J. Clin. Biochem. Nutr.* **2010**, *47*, 181–190. [CrossRef]
10. Kawashima, T.; Ohkubo, K.; Fukuzumi, S. Radical Scavenging Reactivity of Catecholamine Neurotransmitters and the Inhibition Effect for DNA Cleavage. *J. Phys. Chem. B* **2010**, *114*, 675–680. [CrossRef]
11. Landino, L.M.; Shuckrow, Z.T.; Mooney, A.S.; Lauderback, C.O.; Lorenzi, K.E. Photo-Oxidation and Photoreduction of Catechols by Chlorophyll Metabolites and Methylene Blue. *Chem. Res. Toxicol.* **2022**, *35*, 1851–1862. [CrossRef] [PubMed]
12. Segura-Aguilar, J.; Paris, I.; Muñoz, P.; Ferrari, E.; Zecca, L.; Zucca, F.A. Protective and Toxic Roles of Dopamine in Parkinson's Disease. *J. Neurochem.* **2014**, *129*, 898–915. [CrossRef] [PubMed]

13. Young, A.R.; Morgan, K.A.; Harrison, G.I.; Lawrence, K.P.; Petersen, B.; Wulf, H.C.; Philipsen, P.A. A Revised Action Spectrum for Vitamin D Synthesis by Suberythemal UV Radiation Exposure in Humans in Vivo. *Proc. Natl. Acad. Sci. USA* **2021**, *118*, e2015867118. [CrossRef] [PubMed]
14. Ivanova, D.; Zhelev, Z.; Getsov, P.; Nikolova, B.; Aoki, I.; Higashi, T.; Bakalova, R. Vitamin K: Redox-Modulation, Prevention of Mitochondrial Dysfunction and Anticancer Effect. *Redox Biol.* **2018**, *16*, 352–358. [CrossRef] [PubMed]
15. Davies, G.; Ghabbour, E.A.; Steelink, C. Humic Acids: Marvelous Products of Soil Chemistry. *J. Chem. Educ.* **2001**, *78*, 1609. [CrossRef]
16. Sun, Y.; Pham, A.N.; Hare, D.J.; Waite, T.D. Kinetic Modeling of pH-Dependent Oxidation of Dopamine by Iron and Its Relevance to Parkinson's Disease. *Front. Neurosci.* **2018**, *12*, 859. [CrossRef] [PubMed]
17. de Grey, A.D.N.J. HO_2•: The Forgotten Radical. *DNA Cell Biol.* **2002**, *21*, 251–257. [CrossRef] [PubMed]
18. Kalyanaraman, B.; Sealy, R.C.; Liehr, J.G. Characterization of Semiquinone Free Radicals Formed from Stilbene Catechol Estrogens: An ESR Spin Stabilization and Spin Trapping Study. *J. Biol. Chem.* **1989**, *264*, 11014–11019. [CrossRef] [PubMed]
19. Lopes, G.R.; Pinto, D.C.G.A.; Silva, A.M.S. Horseradish Peroxidase (HRP) as a Tool in Green Chemistry. *RSC Adv.* **2014**, *4*, 37244–37265. [CrossRef]
20. Veitch, N.C. Horseradish Peroxidase: A Modern View of a Classic Enzyme. *Phytochemistry* **2004**, *65*, 249–259. [CrossRef]
21. Bisaglia, M.; Mammi, S.; Bubacco, L. Kinetic and Structural Analysis of the Early Oxidation Products of Dopamine: Analysis of the Interactions with α-Synuclein. *J. Biol. Chem.* **2007**, *282*, 15597–15605. [CrossRef] [PubMed]
22. Napolitano, A.; Crescenzi, O.; Pezzella, A.; Prota, G. Generation of the Neurotoxin 6-Hydroxydopamine by Peroxidase/H_2O_2 Oxidation of Dopamine. *J. Med. Chem.* **1995**, *38*, 917–922. [CrossRef] [PubMed]
23. Mukai, K.; Morimoto, H.; Kikuchi, S.; Nagaoka, S. Kinetic Study of Free-Radical-Scavenging Action of Biological Hydroquinones (Reduced Forms of Ubiquinone, Vitamin K and Tocopherol Quinone) in Solution. *Biochim. Biophys. Acta (BBA) General. Subj.* **1993**, *1157*, 313–317. [CrossRef]
24. Hessler, D.P.; Frimmel, F.H.; Oliveros, E.; Braun, A.M. Solvent Isotope Effect on the Rate Constants of Singlet-Oxygen Quenching by Edta and Its Metal Complexes. *Helv. Chim. Acta* **1994**, *77*, 859–868. [CrossRef]
25. Ferroud, C.; Rool, P.; Santamaria, J. Singlet Oxygen Mediated Alkaloid Tertiary Amines Oxidation by Single Electron Transfer. *Tetrahedron Lett.* **1998**, *39*, 9423–9426. [CrossRef]
26. Ferruzzi, M.G.; Blakeslee, J. Digestion, Absorption, and Cancer Preventative Activity of Dietary Chlorophyll Derivatives. *Nutr. Res.* **2007**, *27*, 1–12. [CrossRef]
27. Ma, L.; Dolphin, D. The Metabolites of Dietary Chlorophylls. *Phytochemistry* **1999**, *50*, 195–202. [CrossRef]
28. Eichwurzel, I.; Stiel, H.; Röder, B. Photophysical Studies of the Pheophorbide a Dimer. *J. Photochem. Photobiol. B Biol.* **2000**, *54*, 194–200. [CrossRef] [PubMed]
29. McCord, J.M.; Fridovich, I. Superoxide Dismutase: The First Twenty Years (1968–1988). *Free. Radic. Biol. Med.* **1988**, *5*, 363–369. [CrossRef]
30. Davies, M.J. Singlet Oxygen-Mediated Damage to Proteins and Its Consequences. *Biochem. Biophys. Res. Commun.* **2003**, *305*, 761–770. [CrossRef]
31. Beckman, J.S.; Siedow, J.N. Bactericidal Agents Generated by the Peroxidase-Catalyzed Oxidation of Para-Hydroquinones. *J. Biol. Chem.* **1985**, *260*, 14604–14609. [CrossRef]
32. Meng, X.-G.; Guo, Y.; Hu, C.-W.; Zeng, X.-C. Mimic Models of Peroxidase—Kinetic Studies of the Catalytic Oxidation of Hydroquinone by H_2O_2. *J. Inorg. Biochem.* **2004**, *98*, 2107–2113. [CrossRef] [PubMed]
33. Ogilby, P.R. Singlet Oxygen: There Is Indeed Something New under the Sun. *Chem. Soc. Rev.* **2010**, *39*, 3181–3209. [CrossRef] [PubMed]
34. Harbour, J.R.; Issler, S.L. Involvement of the Azide Radical in the Quenching of Singlet Oxygen by Azide Anion in Water. *J. Am. Chem. Soc.* **1982**, *104*, 903–905. [CrossRef]
35. Ferrari, R.P.; Laurenti, E.; Casella, L.; Poli, S. Oxidation of Catechols and Catecholamines by Horseradish Peroxidase and Lactoperoxidase: ESR Spin Stabilization Approach Combined with Optical Methods. *Spectrochim. Acta Part. A Mol. Spectrosc.* **1993**, *49*, 1261–1267. [CrossRef]
36. Hartley, C.L.; DiRisio, R.J.; Screen, M.E.; Mayer, K.J.; McNamara, W.R. Iron Polypyridyl Complexes for Photocatalytic Hydrogen Generation. *Inorg. Chem.* **2016**, *55*, 8865–8870. [CrossRef]
37. Pellegrin, Y.; Odobel, F. Les Donneurs d'électron Sacrificiels Pour La Production de Combustible Solaire. *Comptes Rendus Chim.* **2017**, *20*, 283–295. [CrossRef]
38. Sueishi, Y.; Hori, M.; Ishikawa, M.; Matsu-Ura, K.; Kamogawa, E.; Honda, Y.; Kita, M.; Ohara, K. Scavenging Rate Constants of Hydrophilic Antioxidants against Multiple Reactive Oxygen Species. *J. Clin. Biochem. Nutr.* **2014**, *54*, 67–74. [CrossRef]
39. Tardivo, J.P.; Del Giglio, A.; De Oliveira, C.S.; Gabrielli, D.S.; Junqueira, H.C.; Tada, D.B.; Severino, D.; De Fátima Turchiello, R.; Baptista, M.S. Methylene Blue in Photodynamic Therapy: From Basic Mechanisms to Clinical Applications. *Photodiagnosis Photodyn. Ther.* **2005**, *2*, 175–191. [CrossRef]
40. Hak, A.; Ali, M.S.; Sankaranarayanan, S.A.; Shinde, V.R.; Rengan, A.K. Chlorin e6: A Promising Photosensitizer in Photo-Based Cancer Nanomedicine. *ACS Appl. Bio Mater.* **2023**, *6*, 349–364. [CrossRef]
41. Abrahamse, H.; Hamblin, M.R. New Photosensitizers for Photodynamic Therapy. *Biochem. J.* **2016**, *473*, 347–364. [CrossRef]

42. Dąbrowski, J.M. Chapter Nine—Reactive Oxygen Species in Photodynamic Therapy: Mechanisms of Their Generation and Potentiation. *Adv. Inorg. Chem.* **2017**, *70*, 343–394. [CrossRef]
43. Dutta, S.; Ruehle, J.; Schikora, M.; Deussner-Helfmann, N.; Heilemann, M.; Zatsepin, T.; Duchstein, P.; Zahn, D.; Knoer, G.; Mokhir, A. Red Light-Triggered Photoreduction on a Nucleic Acid Template. *Chem. Commun.* **2020**, *56*, 10026–10029. [CrossRef]
44. Krieger-Liszkay, A. Singlet Oxygen Production in Photosynthesis. *J. Exp. Bot.* **2005**, *56*, 337–346. [CrossRef] [PubMed]
45. Campos-Martin, J.M.; Blanco-Brieva, G.; Fierro, J.L.G. Hydrogen Peroxide Synthesis: An Outlook beyond the Anthraquinone Process. *Angew. Chem. Int. Ed.* **2006**, *45*, 6962–6984. [CrossRef] [PubMed]
46. Hou, H.; Zeng, X.; Zhang, X. Production of Hydrogen Peroxide by Photocatalytic Processes. *Angew. Chem. Int. Ed.* **2020**, *59*, 17356–17376. [CrossRef]